Evidence of speckle in extreme-UV lithography

Alessandro Vaglio Pret,[1,2,*] Roel Gronheid,[1] Jan Engelen,[2] Pei-Yang Yan,[3] Michael J. Leeson,[4] and Todd R. Younkin[1,4]

[1]*IMEC, Kapeldreef 75, B-3001 Leuven, Belgium*
[2]*Katholieke Universiteit Leuven (K.U.Leuven), department of Electrical Engineering (ESAT), Kasteelpark Arenberg 10, B-3001, Heverlee, Belgium*
[3]*Intel Corporation, 3065 Bowers Ave, Santa Clara, CA 95054, USA*
[4]*Intel Corporation, 2501 NW 229th Avenue, Hillsboro, OR 97124, USA*
[*]*vaglio@imec.be*

Abstract: Based on reflective optics at 13.5 nm, extreme-UV lithography is the ultimate top-down technique to define structures below 22 nm but faces several challenges arising from the discrete nature of light and matter. Owing to the short wavelength, mask surface roughness plays a fundamental role in the increase of speckle pattern contrast, compromising the uniformity of the printed features. Herein, we have used a mask with engineered gradient surface roughness to illustrate the impact that speckle has on the resulting photoresist pattern. The speckle increases the photoresist roughness, but surprisingly, only when the mask surface roughness is well above existing manufacturing capabilities.

OCIS codes: (030.6140) Speckle; (110.5220) Photolithography.

References and links

1. ITRS website. *http://www.itrs.net/*.
2. C. Wagner and H. Noreen, "EUV lithography: lithography gets extreme," Nat. Photonics **4**(1), 24–26 (2010).
3. M. Kawata, A. Takada, H. Hayashi, N. Sugimoto, and S. Kikugawa, "Novel low thermal expansion material for EUV application," Proc. SPIE **6151**, 368–374 (2006).
4. R. Hudyma and U. Mann, "Projection system for EUV lithography," U.S. patent 7,355,678 (April 8, 2008). *http://spie.org/samples/PM178.pdf*
5. G. Zhang, P.-Y. Yan, T. Liang, Y. Du, P. Sanchez, S.- Park, E. J. Lanzendorf, C.-J. Choi, E. Y. Shu, A. R. Stivers, J. Farnsworth, K. Hsia, M. Chandhok, M. J. Leeson, and G. Vandentop, "EUV Mask process development and integration," Proc. SPIE **6283**, 62830G, 62830G-10 (2006).
6. J. W. Goodman, *Introduction to Fourier Optics* (Roberts and Company Publishers, 2004), Chap. 6.
7. J. W. Goodman, *Speckle Phenomena in Optics* (Roberts and Company Publishers, 2010), Chaps. 1–3, 6, 8.
8. P. P. Naulleau, C. N. Anderson, L.-M. Baclea-an, P. Denham, S. George, K. A. Goldberg, M. Goldstein, B. Hoef, R. Hudyma, G. Jones, C. Koh, B. La Fontaine, B. McClinton, R. H. Miyakawa, W. Montgomery, J. Roller, and T. W. S. Wurm, "The SEMATECH Berkeley microfield exposure tool: learning at the 22-nm node and beyond," Proc. SPIE **7271**, 7271W (2009).
9. G. M. Gallatin and P. P. Naulleau, "Modeling the transfer of line edge roughness from an EUV mask to the wafer," Proc. SPIE **7969**, 796903, 796903-10 (2011).
10. S. A. George, P. P. Naulleau, E. M. Gullikson, I. Mochi, F. Salmassi, K. A. Goldberg, and E. H. Anderson, "Replicated mask surface roughness effects on EUV lithographic patterning and line edge roughness," Proc. SPIE **7969**, 79690E, 79690E-10 (2011).
11. Y. Ban, S. Sundareswaran, R. Panda, and D. Z. Pan, "Electrical impact of line-edge roughness on sub-45-nm node standard cells," J. Micro/Nanolith. **9**, 6–10 (2010).
12. P. Poliakov, P. Blomme, A. Vaglio Pret, M. M. Corbalan, R. Gronheid, D. Verkest, J. Van Houdt, and W. Dehaene, "Induced variability of cell-to-cell interference by line edge roughness in NAND flash arrays," IEEE Electron Device Lett. **33**(2), 164–166 (2012).
13. P. P. Naulleau, D. Niakoula, and G. Zhang, "System-level line-edge roughness limits in extreme ultraviolet lithography," J. Vac. Sci. Technol. B **26**(4), 1289–1293 (2008).
14. Y. Wei and R. L. Brainard, *Line-Edge Roughness of Resist Patterns in Advanced Processes for 193-Nm Immersion Lithography* (SPIE Press, 2009), Chap. 10.
15. T.-S. Gau and C.-C. Hsia, "Illumination aperture filter design using superposition," U.S. patent 6,361,909 (March 26, 2002). *http://www.google.com/patents/US6361909.*
16. K. Jain, C. G. Willson, B. J. Lin, and B. J, "Fine-line high-speed excimer laser lithography," Symposium on VLSI Technology, Digest of Technical Papers (1982), pp. 92–93.

#175771 - $15.00 USD Received 7 Sep 2012; revised 15 Oct 2012; accepted 17 Oct 2012; published 2 Nov 2012

17. O. Noordman, T. Andrey, B. Jan, T. James, P. Gary, P. Michael, B. Vladan, and M. Manfred, "Speckle in optical lithography and the influence on line width roughness," J. Micro/Nanolith. **8**, 043002 (2009).
18. G. M. Gallatin, N. Kita, T. Ujike, and B. Partlo, "Residual speckle in a lithographic illumination system," J. Micro/Nanolith. MEMS MOEMS **8**, 043003 (2009).
19. C. N. Anderson and P. P. Naulleau, "Do not always blame the photons: relationships between deprotection blur, line-edge roughness, and shot noise in extreme ultraviolet photoresists," J. Vac. Sci. Technol. B **27**(2), 665–670 (2009).
20. C. A. Mack, J. W. Thackeray, J. J. Biafore, and M. D. Smith, "Stochastic exposure kinetics of EUV photoresists: a simulation study," J. Micro/Nanolith. **10**, 033019 (2011).
21. C. A. Mack, *Fundamental Principles of Optical Lithography* (Wiley & Sons, 2007), Chaps. 5–7.
22. P. P. Naulleau and G. M. Gallatin, "Line-edge roughness transfer function and its application to determining mask effects in EUV resist characterization," Appl. Opt. **42**(17), 3390–3397 (2003).
23. V. Constantoudis, G. P. Patsis, A. Tserepi, and E. Gogolides, "Quantification of line-edge roughness of photoresists. II. Scaling and fractal analysis and the best roughness descriptors," J. Vac. Sci. Technol. B **21**(3), 1019–1026 (2003).
24. S. A. George, P. P. Naulleau, F. Salmassi, I. Mochi, E. M. Gullikson, K. A. Goldberg, and E. H. Anderson, "Extreme ultraviolet mask substrate surface roughness effects on lithographic patterning," J. Vac. Sci. Technol. B **28**, C6E23–C6E30 (2010).
25. H.-J. Mann, "Six-mirror EUV projection system with low incidence angles," U.S. patent 7,973,908 (July 5, 2011). *http://www.google.com/patents/US20090079952*.
26. A. Vaglio Pret, R. Gronheid, T. Ishimoto, and K. Sekiguchi, "Resist roughness evaluation and frequency analysis: metrological challenges and potential solutions for extreme ultraviolet lithography" J. Micro/Nanolith. **9**, 041308 (2010).
27. A. R. Pawloski, A. Acheta, I. Lalovic, B. M. La Fontaine, and H. J. Levinson, "Characterization of line-edge roughness in photoresist using an image fading technique," Proc. SPIE **5376**, 414–425 (2004).
28. C. Vassilios, G. P. Patsis, and E. Gogolides, "Photoresist line-edge roughness analysis using scaling concepts," J. Micro/Nanolith. **3**, 429–435 (2004).
29. A. K. K. Wong, *Resolution Enhancement Techniques in Optical Lithography* (SPIE Press, 2001), Chaps. 2–4.
30. C. Rydberg, J. Bengtsson, and T. Sandström, "Performance of diffractive optical elements for homogenizing partially coherent light," J. Opt. Soc. Am. A **24**(10), 3069–3079 (2007).

1. Introduction

Extreme UV (EUV) lithography is still the primary candidate to allow scaling below the 22 nm technology node for semiconductor manufacturing [1]. This soft x-ray lithography uses a relatively coherent radiation generated by a discharge-produced Tin (Sn) plasma source at 13.5 nm [2]. Due to the high absorbance of matter at this wavelength, all the optical elements are Bragg-reflectors. The mask is composed of reflective elements upon a flat LTEM support (Low Thermal Expansion Material) [3] whereupon 40 Molybdenum/Silicon (Mo/Si) interference bilayers are deposited to achieve 70% reflectivity [4]. On top of the multilayer, a 2-3 nm protective layer of Ruthenium (Ru) is deposited (Fig. 1(a)). Both the multilayer and Ru layer are characterized by a certain surface roughness [5].

During exposure, the mask reflects EUV light from the source to the optics and then to the wafer which has a photosensitive film (photoresist) coated on top. In this process, the Mask Surface Roughness (MSR) acts as a diffuser, leading to the creation of speckle pattern due to local phase mismatch [6]. The contrast of a speckle pattern depends on several factors: the wavelength, the spatial and temporal coherence of the source, and the optical system flatness and design [7]. However, for EUV lithography systems, concern arises mainly from speckle stemming from MSR [8,9]. Correlated scatter coming from a phase coherent substrate that propagates through the multilayer system until the protective layer has been shown to lead to random phase errors. In addition, although of lower magnitude, uncorrelated scatter from the interface roughness between the Mo/Si layers needs to be taken into account for local reflectivity variation across the mask [10]. Combined, these effects lead to local intensity fluctuations at the wafer level which cause roughness formation during the definition of the edges of the features. This is of concern, since at the targeted dimensions pattern roughness has become one of the major contributions to electrical device failures [11, 12].

#175771 - $15.00 USD Received 7 Sep 2012; revised 15 Oct 2012; accepted 17 Oct 2012; published 2 Nov 2012

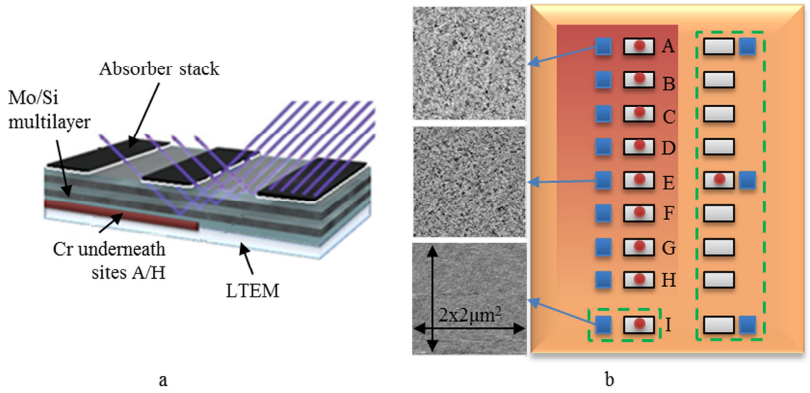

Fig. 1. (a) Cartoon of an EUV mask representing the absorber stack, the Mo/Si multilayer, the Cr layer for surface roughness variation, the LTEM substrate, and the EUV light path. (b) Mask layout used for speckle evaluation: the red area represents the Cr layer deposited to increase the surface roughness (labeled from A to H), the white rectangles represent the locations of the mask gratings (54 nm line/space, 1:1 duty cycle), the red dots are the top-down SEM picture locations on wafer, and the green dashed lines indicate the reference modules (no Cr deposited, I site). On the left, AFM images for high, mid and low surface roughness are reported.

Recent works show that to print structures at 22 nm half pitch and below, speckle phenomena are foreseen to impact the LER for MSR higher than 50 pm rms [1,13]. In this work, photoresist Line Edge Roughness (LER) [14] is used to quantify the impact of speckle generated by the MSR during the lithographic exposure of 27 nm line/space feature sizes having a periodicity of 54 nm. In order to quantify the impact of different illuminations on speckle, the LER resulting for Dipole-60 off-axis illumination exposure [15] is compared to Conventional illumination (Figs. 2(a) and 2(b)).

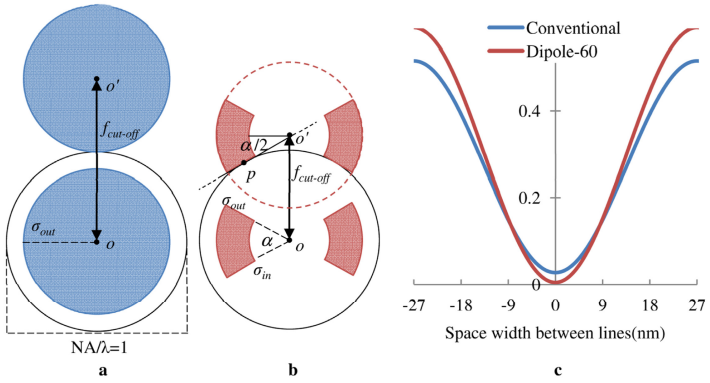

Fig. 2. Sketch of the Conventional (a) and Dipole-60 (b) illuminations used for the exposures. In the cartoons, the + 1 diffraction orders are represented for $f = f_{cut-off}$. c) Aerial image contrast of Conventional (blue) and Dipole-60 (red) illumination for 54 nm line/space exposure.

2. Concept

For previous Deep UV (DUV) optical lithography, speckle is rarely observed due to the highly random mode structure of the excimer laser output (ArF at 193 nm, KrF at 248 nm wavelength) [16]. In fact, only recently, has O. Noordman et al. [17] been able to experimentally determine the impact of speckle on LER using a combination of low number of ArF laser pulses, a high degree of polarization, and off-axis illumination conditions. Speckle pattern contrast is given by Eq. (1) [17, 18]:

#175771 - $15.00 USD Received 7 Sep 2012; revised 15 Oct 2012; accepted 17 Oct 2012; published 2 Nov 2012

$$Speckle\ pattern\ contrast \propto \sqrt{\frac{1}{N_p}}\sqrt{\frac{\lambda^2}{G}+\frac{\tau_c}{T}} \qquad \tau_c = \frac{1}{2\pi c}\frac{\lambda^2}{\Delta\lambda} \qquad (1)$$

where N_p is the number of polarized states, T is the length of the laser pulse, τ_c is the laser temporal coherence, and G is a factor related to its spatial coherence and geometric properties of the light. It is noticed that the speckle contrast on EUV lithography is expected to be less severe compared to ArF lithography for several reasons: lack of polarization for EUV light (Np_{EUV} / Np_{ArF} ≈2), high T due to different light sources (T_{EUV} / T_{ArF} ≈100), small wavelength and particularly broad band (the factor $\lambda^2/\Delta\lambda$ in τ_c is roughly 10^4 higher for ArF laser).

Photoresist materials capture the speckle pattern as a discrete Poisson distribution of photons [19] to photo-generate a quasi-Poisson distribution of acids [20] which will be responsible for polymer deprotection and the subsequent dissolution switch [21]. Hence, the speckle effect will be seen by the photoresist as a local intensity variation, increasing or decreasing the photon density, acid generation, deprotection, and dissolution into developer. For these reasons, we decided to investigate how the intensity fluctuations induced by the speckle impact the roughness of printed features in EUV lithography.

To evaluate the speckle contribution, a mask with a controlled MSR gradient has been used for lithographic exposure. Due to its large-scale intensity fluctuations and the optical system illumination-dependent cut-off, an increase of low-frequency LER is expected for the features defined in the photoresist up to the spatial frequency cut-off [17]. Performing Power Spectral Density (PSD) analysis of LER frequencies of the vertical line edges [22, 23], we can experimentally observe the speckle impact on photoresist due to MSR.

2. Experiment

2.1 Experimental settings

In order to evaluate the speckle effect originated by MSR, a special mask with a surface roughness gradient was prepared in collaboration with Intel, Sematech, and LBNL [5]. After the preparation of the LTEM support, a layer of Chromium (Cr) (Fig. 1, red area) was deposited on part of the mask to aggravate the surface roughness in a controlled way [10]. The fabrication procedure involved the shadowed deposition of the Cr layer. The deposition was completed using DC magnetron sputtering in an Argon gas environment [10]. The shadowing was controlled to produce a roughness gradient in one direction only (Fig. 1(b)). The right half side of the mask served as reference location. As illustrated in Fig. 1(b), Atomic Force Microscopy (AFM) mask surface measurements were performed along the aggravated surface roughness as indicated by the blue squares on the mask layout. In Table 1, AFM MSR values are reported: surface roughness varied from more than 1000 pm rms (roughest area, site A) down to 60 pm rms for the reference case, reflecting the natural roughness of the substrate (no Cr layer deposition, site I). EUV reflectivity measurements were performed and a significant reflectivity drop was noted with increased MSR (Table 1). These values closely match those reported by S. A. George et al. in previous studies [10,24]. AFM measurements were taken in tapping mode, with a Tespa tip, scan speed of 2 μm/sec and a resolution of 256 lines/image, 256 pts/line on 2x2 μm^2 areas. Measurement repeatability is estimated to be 20 pm.

Table 1. AFM MSR and mask reflectivity measurements along the mask area where Cr is deposited to aggravate the resulting surface roughness. Measurements errors are respectively 20 pm and 0.08%.

Mask site	A	B	C	D	E	F	G	H	I (ref.)
AFM rms (pm)	1110	970	850	740	600	480	220	90	60
Mask Reflectivity (%)	51.9	54.5	57.4	59.8	62.0	63.2	64.1	64.5	64.6

#175771 - $15.00 USD Received 7 Sep 2012; revised 15 Oct 2012; accepted 17 Oct 2012; published 2 Nov 2012

In Fig. 1(b), the white rectangles indicate the locations of the 27 nm line/space gratings having a periodicity of 54 nm (1:1 duty cycle) which were exposed for speckle evaluation: the red dots represent the locations on the wafer where top-down Scanning Electron Microscopy (SEM) images were captured to perform LER analysis in the photoresist. The green dashed lines indicate the reference modules without Cr layer deposition (reference MSR = 60 pm rms). Measuring the LER in photoresist along the aggravated MSR will provide the relationship between LER and MSR due to speckle pattern contrast, and photoresist performance.

The mask was hence exposed with the imec NXE:3100 ASML EUV tool equipped with a USHIO/XTREME DPP EUV source (λ = 13.5, Numerical Aperture NA = 0.25). Illumination system details are reported in [25]. Two illumination conditions were used: Conventional with a coherence factor σ_{out} = 0.81 (Fig. 2(a)), and Dipole-60 with poles of α = 60° distributed horizontally in the pupil and σ_{in} = 0.43, σ_{out} = 0.81 (Fig. 2(b)). The optical system frequency cut-off represents the higher frequency (shorter periodicity) for which the 1st diffraction order is still collected by the pupil. As represented in Fig. 2, the cut-off is illumination dependent.

In the exposure experiment, 40 nm thickness of commercial EUV photoresist SEVR140 from SEC were spin-coated on 300 mm Si wafers. The wafers were pre-treated by spin-coating 20 nm organic underlayer AL412 from Brewer Science. A HITACHI CG4000SEM was used to perform pattern analysis. Out of focus conditions of respectively −50 nm and −30 nm (focus plane below the wafer surface) were used to increase the speckle contribution to photoresist LER [10]. 27 nm line/space gratings with a periodicity of 54 nm (1:1 duty-cycle) were exposed on the wafer with different MSR to evaluate the speckle contribution to photoresist LER. In order to fully capture the speckle effect on printed features, and fulfill the ITRS specifications [1], top-down SEM micrographs were captured with an asymmetric field of view: 0.45 μm in direction perpendicular to the lines was used to have enough details on the protrusions and the roughness of the edges, while 2.25 μm was chosen along the lines to also collect the low-frequency roughness component. 18 images with 7 lines/image were considered for each MSR module to increase the accuracy of the measurement and decrease the noise of the PSD analysis [26]. With the chosen SEM setting, LER SEM noise measurement was estimated to be less than 0.1 nm (3σ)

2.2 Experimental quantification of speckle on photoresist roughness

Exposure intensity variations from MSR are expected to impact the LER performance of the printed features [13,22]. In addition, the impact of the effect is predicted to increase with higher spatial coherence. To evaluate both the predictions, two wafers were exposed with Conventional (low spatial coherence, Fig. 2(a)) and Dipole-60 illuminations (high spatial coherence, Fig. 2(b)). In order to define 27 nm line/space with 54 nm periodicity at wafer level, the exposure energy was varied for different MSR (Fig. 3(a)).

The required exposure energy increase to obtain the target feature dimensions is explained by considering the reflectivity drop for higher MSR (Table 1): to define the same feature dimension into the photoresist, the same number of photons must be absorbed; for higher MSR the intensity loss due to photon scattering and phase mismatch is higher, hence the average intensity at wafer level is reduced. The reflectivity drop can be noticed starting with MSR = 90 pm rms, which requires higher energy compared to the reference case (MSR = 60 pm). The exposure energies for the Dipole-60 illumination are generally lower than for the Conventional due to higher contrast of the aerial image for the Dipole-60 (Fig. 2(c)).

In Fig. 3(b), the trends for photoresist LER are reported as a function of MSR (reported in nm, 3σ): the speckle contribution is clearly visible for MSR>500 pm rms. This is also evident from the different SEM micrographs reported in Figs. 3(c) and 3(d): for MRS = 1110 nm rms bridging between lines is noticed. LER variations for structures with MRS below 480 nm are considered within the measurement error [26]. The higher aerial image contrast is responsible for the overall lower LER for lines exposed with the Dipole-60 off-axis illumination [27].

#175771 - $15.00 USD Received 7 Sep 2012; revised 15 Oct 2012; accepted 17 Oct 2012; published 2 Nov 2012

2.3 Speckle response to different illumination settings

To verify that the detrimental effect on LER is effectively caused by the speckle effect, PSD analysis of photoresist edges was performed with LERDEMO software by Demokritos [28]. Using Fourier analysis, and knowing that different illuminations have a different frequency cut-off, we are able to quantify any roughness variation due to the speckle effect in the frequency domain. For the Conventional case, the frequency cut-off is given by the Rayleigh principle which defines the theoretical resolution limit of a lithographic optical system [29]:

$$f_{cut-off}\left(Conventional\right)=\frac{NA}{\lambda}\left(1+\sigma_{out}\right)=34\mu m^{-1} \tag{2}$$

For the Dipole-60, the $f_{cut\text{-}off}$ can be found solving the system for the tangency condition (point p of Fig. 2(b)) between a straight line with m = 0.5 ($sin(\alpha/2)$ with α = 60) and the circumference (pupil) centered in $o(0,0)$ and radius 1 (NA/ λ):

$$\begin{cases} y=mx+q \\ x^2+y^2=1 \end{cases} \tag{3}$$

The tangency condition is found for the positive q:

$$q=\mp\sqrt{\left(m^2+1\right)}\rightarrow q=\frac{\sqrt{5}}{2}\rightarrow f_{cut-off}\left(Dipole\right)=q\frac{NA}{\lambda}=20.7\mu m^{-1} \tag{4}$$

For the considered illumination, using Eqs. (2) and (4), it is so possible to demonstrate that:

$$f_{cut-off}\left(Conventional\right)=34\mu m^{-1} \qquad f_{cut-off}\left(Dipole60\right)=20.7\mu m^{-1} \tag{5}$$

#175771 - $15.00 USD Received 7 Sep 2012; revised 15 Oct 2012; accepted 17 Oct 2012; published 2 Nov 2012

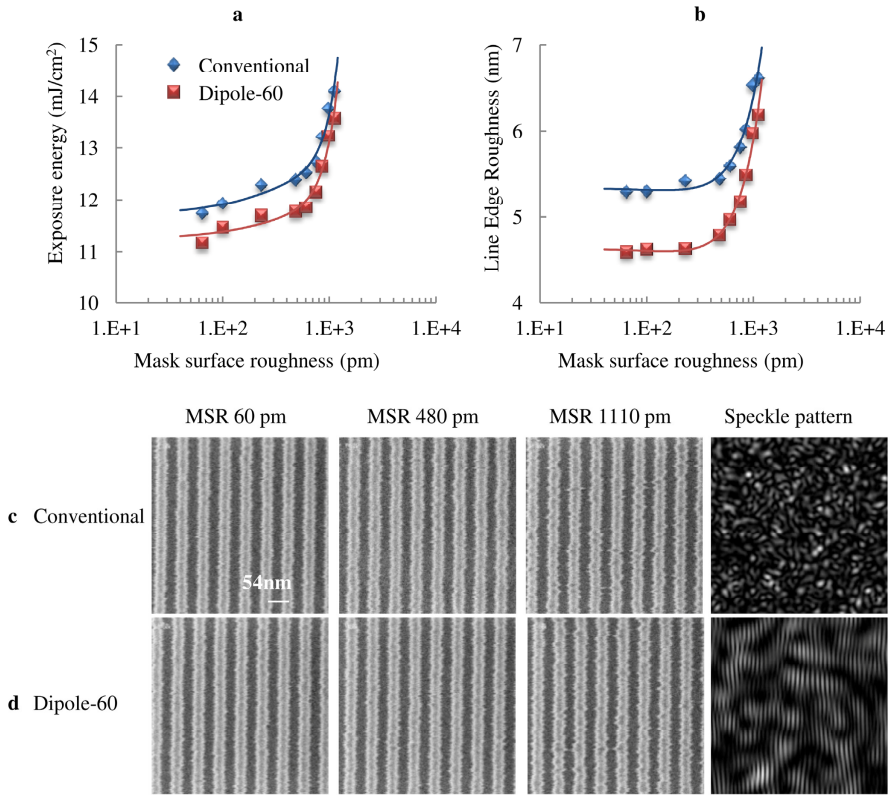

Fig. 3. (a) Exposure energies and (b) LER upon mask surface roughness for Conventional (blue) and Dipole-60 (red) illumination. Below, top-down SEM micrographs for 54 nm line/space gratings exposed with (c) Conventional and (d) Dipole-60 illumination at different mask surface roughness. On the right, the speckle patterns are also shown [18].

In Fig. 4, the PSD analyses performed on SEM micrographs of photoresist lines exposed with Conventional and Dipole-60 illuminations are illustrated for the 9 different MSR modules considered. By using the Parseval theorem for Discrete Fourier Transform analysis, it can be show that the area subtended by each PSD curve is proportional to LER^2 reported in Fig. 3(b). For both graphs, it is observed that the speckle effect caused by the aggravated MSR increases the PSD amplitudes just for the frequencies below the cut-off.

We have also been able to capture a second effect due to the different speckle patterns generated by Conventional and Dipole-60 illuminations. The speckle pattern is strongly illumination shape-dependent [7,18,30]. Due to the intensity distribution in the pupil, the speckle pattern for Conventional illumination is expected to vary in size as well as orientation due to its circle-symmetry, while for Dipole-60 illumination the size variation is limited because of its smaller size and is characterized by a privileged orientation perpendicular to the poles arising from the limited angular distribution in the pupil [18, 30]. Moreover, due to the higher spatial coherence, the speckle contrast for Dipole-60 illumination is higher than for Conventional case (Figs. 3(c) and 3(d), right). This is reflected in a more pronounced effect on LER in the photoresist. In the graph of Fig. 5, the variation of LER is plotted as a function of the exposure intensity variation, both normalized to the reference MSR case. Through a linear fit, it is possible to see how the slope for the Conventional illumination is slightly but clearly lower when compared to the Dipole-60. This demonstrates that a more performing off-axis illumination can increase the speckle contrast, resulting in an aggravated LER response.

#175771 - $15.00 USD Received 7 Sep 2012; revised 15 Oct 2012; accepted 17 Oct 2012; published 2 Nov 2012

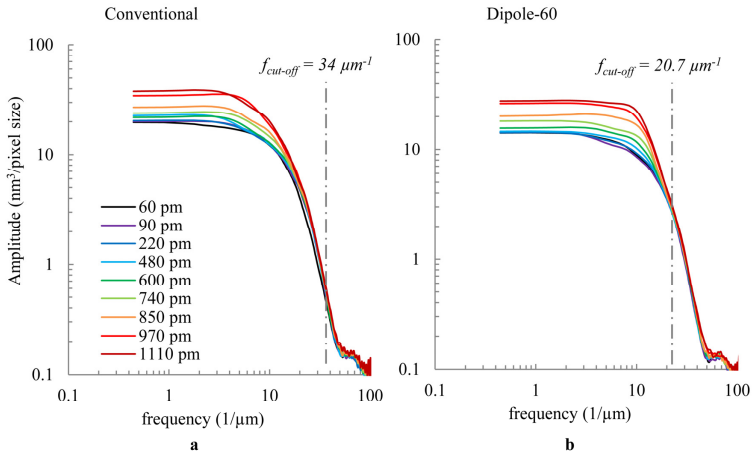

Fig. 4. PSD analysis of line edge roughness for 54 nm line/space gratings exposed with (a) Conventional and (b) Dipole-60 illuminations. The black line correspond to the reference modules (AFM = 60 pm), the other mask surface roughness conditions are represented following the roygbiv color code from violet (low rms) to red (high rms). The dashed grey lines represent the $f_{cut\text{-}off}$ for each illumination condition.

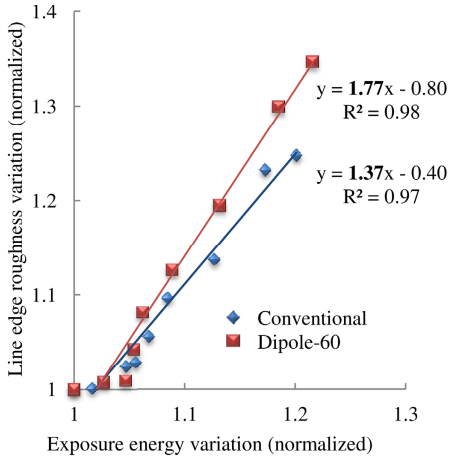

Fig. 5. LER variations upon exposure energy variation normalized on the reference case for Conventional (blue) and Dipole-60 (red) illumination. The solid lines represent a linear fitting of the data. In the graph, fitting equation and R^2 values are also reported.

3. Discussion

The surface roughness of an extreme UV mask increases the speckle patterning contrast due to optical path mismatch and random phase errors of the extreme UV light reflected by the mask used to print nanoscale features on a wafer. With the engineered mask presented in this work, we have been able to quantify the speckle effect for lithographic EUV exposures in the state-of-the-art photoresist material.

As shown in Fig. 3, high mask surface roughness gives rise to two primary effects. First, it decreases the number of photons at the wafer level for a given source power, and secondly, it increases the photoresist roughness, thereby compromising the lithographic performance.

The experimental results obtained with two illumination shapes allow us to capture two other important effects. First, performing a Fourier analysis of the line edge roughness allows us to discriminate the illumination-dependent frequency cut-off (Eq. (5)) of the speckle effect.

#175771 - $15.00 USD Received 7 Sep 2012; revised 15 Oct 2012; accepted 17 Oct 2012; published 2 Nov 2012

Second, the speckle effect increases line edge roughness more rapidly for the Dipole-60 compared to the Conventional illumination (Fig. 5).

The method presented above allowed us to capture the speckle phenomenon performing frequency analysis on top-down SEM feature images. The results qualitatively confirmed the predictions made in previous works. However, the quantitative impact of the speckle effect on line edge roughness is less than expected. The simulations predict a non-negligible speckle contribution to the photoresist roughness for mask surface roughness higher than 50 pm, but in our experiments the photoresist performance starts degrading for mask surface roughness values 10 times higher.

Considering the main challenges which extreme UV lithography must still overcome in order to be considered viable for high volume manufacturing, this work reveals that a further improvement of existing mask manufacturing processes will likely not be translated in improvement of line edge roughness in photoresist pattern.

Acknowledgments

The authors would like to thank Darko Trivkovic and Rik Jonckheere (imec) for mask layout preparation and mask handling for NXE:3100 exposures; Robert Chen (Intel) for AFM measurements, Ken Buckmann and Marylin Kamna (Intel) for mask tape-out and e-beam data preparation; Eric Gullikson and Farhad Salmasi (LBLN) for Cr layer deposition; Vibhu Jindal, Jaewoong Sohn (Sematech) and Andy Ma (Intel) for Mo/Si multilayer deposition. At last, we would like to thank Gregg Gallatin (NIST), Oscar Noordman (ASML) and Marco Ornigotti (MPL) for fruitful discussions.

#175771 - $15.00 USD Received 7 Sep 2012; revised 15 Oct 2012; accepted 17 Oct 2012; published 2 Nov 2012